

IMPLEMENTATION OF MULTI-ENERGY EXTRACTION CONFIGURATIONS AT MEDAUSTRON

K. Holzfeind*, E. Renner, TU Wien, Vienna, Austria
F. Plassard, EBG MedAustron GmbH, Wiener Neustadt, Austria

Abstract

Moving from extracting one single energy per cycle to multiple energies promises improvements in time and power budgets of medical synchrotrons. To ensure reproducible and accurate beams for treatment, hysteresis effects must be considered. To avoid losses during energy changes, the beam has to be moved away from the extraction resonance. Different methods of moving the working point were compared regarding their robustness, adaptability and speed by means of measurements and Xsuite simulations. The measurements were taken at the synchrotron facility MedAustron. The methods are devised for the PIMMS-based lattice with one resonant sextupole and off-momentum operation, and differ in how the working point is shifted during the energy change regarding the timing of element ramps and off-momentum contributions.

INTRODUCTION

The synchrotron-based ion beam treatment and research center MedAustron, based on the Proton Ion Medical Machine Study (PIMMS) [1, 2], provides 62 - 252 MeV proton and 120 - 402 MeV u^{-1} carbon ion beams ($^{12}C^{6+}$) for irradiation of cancer patients. The center further delivers different beam modalities to nonclinical research users. These include the clinical beam modalities as well as low-flux beams, 800 MeV protons and helium ion beams. Ion beam therapy exploits the *Bragg peak* of heavy, charged particles in tissue for highly conformal radiation doses. To modify the penetration depth of the Bragg peak, the energy of the incoming ion beam must be adapted. Nominally, synchrotron operation for patient treatment follows the subsequent workflow: Multiturn injection and acceleration to the energy specified in the treatment plan, followed by betatron core-driven 3rd-order resonant slow extraction [3] until the prescribed dose is delivered. The process concludes with the dumping of any unused beam and conditioning the beamline for the following injection.

In recent years radio frequency knockout (RFKO) [4] has been investigated as alternative slow extraction mechanism at MedAustron [5, 6]. RFKO has some advantages compared to betatron core-driven extraction, such as the compatibility with dynamic intensity control [7], and multi-energy extraction (MEE). With MEE the prescribed dose for several energy slices of the treatment plan can be delivered within one cycle of the synchrotron by re-acceleration or deceleration of the beam after each extraction phase. MEE could shorten the duration of patient treatment significantly and reduce power consumption. This proceeding will report on the

current progress of first experimental tests of RFKO MEE at MedAustron. The ongoing studies focus on loss mitigation during the energy changes, including ensuring robustness in failure scenarios. In this context, different methods for increasing the stable phase space area during these energy ramps are presented and discussed.

STABLE AREA DURING ENERGY RAMPS

For slow extraction at MedAustron, the $3Q_x = 5$ resonance is excited by powering one resonant sextupole. Its normalized strength

$$S = \frac{1}{2} \beta_x^{3/2} k_2 l, \quad (1)$$

depends on the horizontal beta-function at the location of the sextupole β_x , its length l and the normalized sextupole magnet gradient k_2 . The resonance separates the phase space in regions, where particle perform stable or unstable motion. The area of the stable region,

$$A = \frac{48\sqrt{3}\pi^2}{S^2} (\delta Q)^2, \quad (2)$$

is directly proportional to the square of tune distance from the resonance, $\delta Q = Q_{\text{particle}} - Q_{\text{resonance}}$, and inversely proportional to the square of the normalized sextupole strength S . In order to avoid losses during the energy change the stable area in the horizontal phase space should increase compared to the beam's emittance.

Methods

There are various ways of how this can be achieved. Firstly one can weaken the resonance by decreasing the normalized sextupole gradient k_2 , method (a). For $S \gg 1$, the stable area is can also be effectively increased by changing δQ (method (b) - (d)).

Evidently, the resonance can be excited and diminished by (a) turning the resonance driving sextupole on and off. Up to 50 ms will be added to the energy change duration as they are needed for the full resonant sextupole ramp. However, the resonance can also be weakened instead of completely turned off. An example for one such implementation: When increasing the energy, $\Delta E > 0$, and thus the magnetic rigidity $B\rho$, while delaying the gradient ramp of the resonant sextupole, k_2 decreases (blue line in Fig. 1 (b)).

When focusing on changing the tune distance other methods, such as (b) including dedicated optic magnet ramps to change the tune, (c) ramping the momentum offset via radial loop regulation or (d) addition of a delay to the $B\rho$ -ramp

* katrin.holzfeind@tuwien.ac.at

of the bending dipoles compared to the ramp of the optic magnets, can be used.

While an optics change (b) can easily be implemented, these ramps would require additional time and might cause hysteresis effects for current controlled quadrupoles, as installed at MedAustron. Method (c) can be used to increase δQ through a shift in the beam's frequency and hence momentum in case of non-zero chromaticity. The time needed to smoothly reach the desired momentum offset, and consequently the tune change, has yet to be estimated. Furthermore, RFKO optics often include low horizontal chromaticity, meaning the aperture limits cannot be neglected for changes to the momentum offset in the order of $O(10^{-3})$. In Fig. 2 a first implementation of method (d) is shown with integrated field measurements taken during one re-acceleration step. The time advance is applied to all optic magnets, which ramp simultaneously with the red quadrupole curve. The measurement will be discussed further in the section *Measurements*. Below, we investigate option (d) in more detail, i.e. increasing the size of the stable area during the energy change by introducing a delay between the ramp of the dipole and quadrupole magnets. A detailed merit analysis of the other methods is subject to further studies.

FIRST TESTS FOR ASYNCHRONOUS QUADRUPOLE RAMPING

As the normalized quadrupole strength

$$k_1 = \frac{G}{B\rho} \quad (3)$$

can be calculated from the gradient of the magnet G and the magnetic rigidity, and the gradient curve is scaled to the $B\rho$ -curve, we can estimate the resulting tune shift

$$\delta Q(t) = \frac{1}{4\pi} \oint \beta(s) \delta k_1(s, t) ds \quad (4)$$

from the time-dependent shift in magnet strength

$$\delta k(t) = k(0) \left(\frac{B\rho(t + \Delta t)}{B\rho(t)} - 1 \right). \quad (5)$$

This principle of delayed or advanced ramps can be used for all combinations of settings concerning the tune distance $\delta Q \geq 0$ and energy steps $\Delta E \geq 0$. While most accelerator components are ramped without delay, i.e. together with the bending dipoles (Fig. 1 (a)) changing the starting point of the gradient ramp of the focusing quadrupoles (Fig. 3), ensures an increase of the stable area between the extraction phases. The resonant sextupole is ramped separately, see Fig. 1 (b). Its temporal relation to the dipole magnet ramp depends on $\Delta E \geq 0$ to ensure a stable area increase.

Tracking simulations

In order to test and improve the idea of asynchronous optic ramps first simulations with the tracking tool X_{SUITE} [8] were performed. At MedAustron the current working point

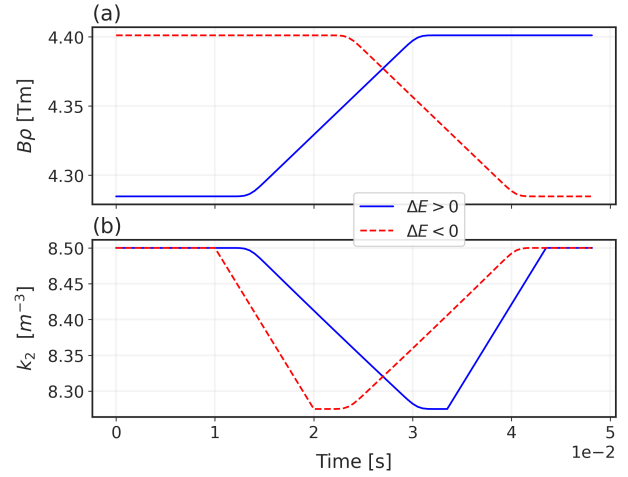


Figure 1: Example of (a) the $B\rho$ -ramp and (b) the resonant sextupole gradient k_2 for increasing and decreasing energy steps, modeled in X_{SUITE}. Blue solid line: $E_{\text{kin}} = 200 - 210 \text{ MeV u}^{-1}$; red dashed line: $E_{\text{kin}} = 210 - 200 \text{ MeV u}^{-1}$ for $^{12}\text{C}^{6+}$ -ions in a modified PIMMS lattice. In the real machine the linear ramp of the resonant sextupole includes round-offs, which are currently not present in the X_{SUITE} model.

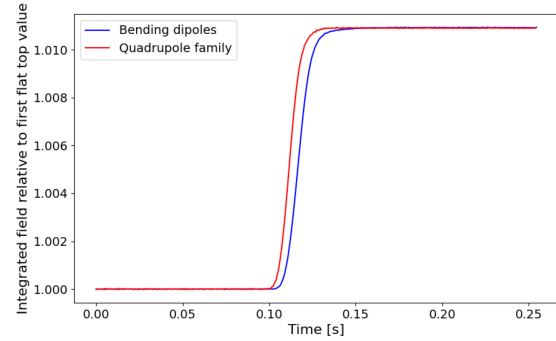


Figure 2: Integrated field for the bending dipoles and one quadrupole family for an energy change from $E_{\text{kin}} = 200 - 204 \text{ MeV u}^{-1}$ for carbon ions. The integrated field is normalized to the corresponding value at $t=0$.

of the experimentally employed, non-clinical RFKO setup lies above the excited $3Q_x = 5$ resonance, at an off-momentum tune of $Q_x \approx 1.673$. Therefore the simulations focus on positive tune distances. A modified PIMMS lattice was used for simulations with 1000 $^{12}\text{C}^{6+}$ -ions. The particles were initialized to fill the outer layer of the stable area A , Eq. (2), for the normalized gradient of a resonant sextupole $k_2 = 8.5 \text{ m}^{-3}$. Furthermore, the beam was initialized as a matched, bunched beam within an RF bucket with the momentum offset $\delta = -2.8 \times 10^{-3}$, voltage $V = 2650 \text{ V}$ and RF frequency $f_{\text{RF}} = (1 - \eta\delta) \times f_0 = 2.26 \text{ MHz}$, where η is the slippage factor and f_0 the on-momentum revolution frequency. The simulation used time-dependent settings, with the dipole and quadrupole ramps illustrated by the blue lines in Fig. 1 (a) and the cyan lines in Fig. 3(b), respectively. The ramp of the focusing quadrupoles was advanced by 1 ms.

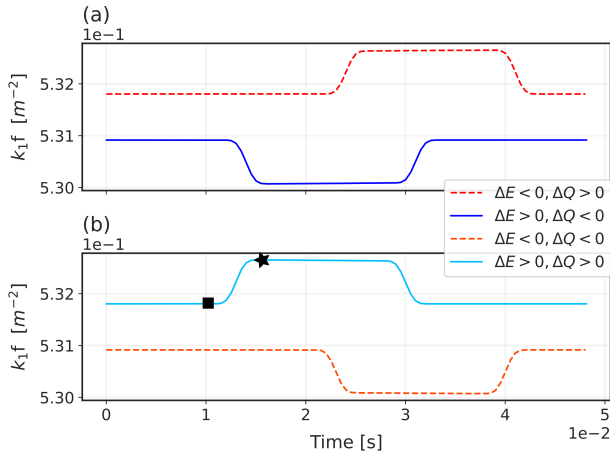


Figure 3: Evolution of focusing quadrupole strength $k_{1,f}$ due to (a) delayed or (b) advanced gradient ramps; modified to ensure an increase of the stable area for combinations of positive and negative tune distances ΔQ and energy steps ΔE . The corresponding $B\rho$ -ramps are shown above.

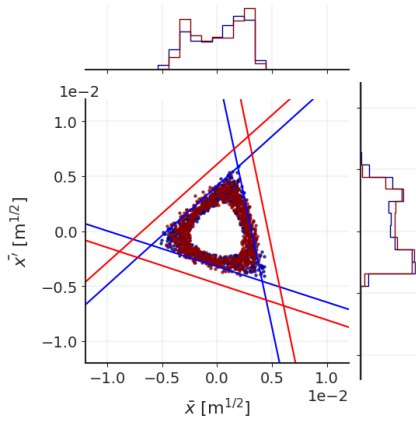


Figure 4: Comparison of particle distribution in normalized, horizontal phase space before the ramp (blue) and the farthest tune shift (red) with the separatrices at the corresponding time stamps.

The resonant sextupole gradient was kept at the previous extraction setting during the energy change and afterwards ramped to achieve the same strength S (blue line in Fig. 1 (b)). All other magnets followed the given $B\rho$ -curve.

In Fig. 4 the normalized phase space is shown at different time instances, depicted in Fig. 3 (b) by ■ and ★. The Kobayashi-Hamiltonian [9, 10] is used to calculate the separatrices, indicating the size of the stable area. The difference in the stable area from before the ramp (blue) to the highest tune distance (in red) is clearly visible. At the highest diversion of k_1 (★ in Fig. 3 (b)) from the matched extraction settings the tunes are shifted by $\Delta Q_x = 3.22 \times 10^{-3}$ and $\Delta Q_y = -1.78 \times 10^{-3}$. After the re-acceleration and the linear ramp of the resonant sextupole's gradient the distribution in horizontal phase space resembles the initial state. Using Eq. (4) leads to expected changes of $\Delta Q_x = 3.35 \times 10^{-3}$ and $\Delta Q_y = -1.84 \times 10^{-3}$ for the maximal difference of the

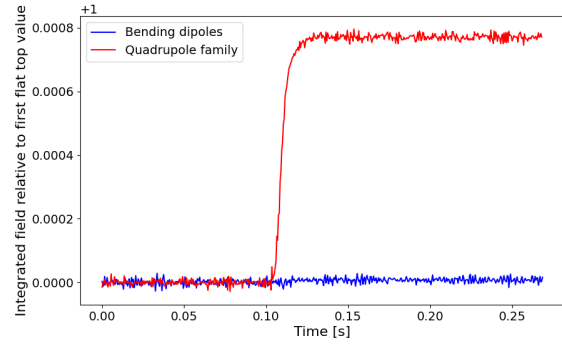


Figure 5: Integrated field for the bending dipoles and one quadrupole family from a custom waveform. The ramp seen in Fig. 2 is interrupted before the bending dipoles start to ramp and a round-off for tune measurements is included.

gradient and $B\rho$ -ramp of $\frac{B\rho(t+\Delta t)}{B\rho(t)} = 1.0016$. Equation (4) shows good agreement between estimation and tracking and can thus be used to calculate the needed delay/ time advance Δt for the desired tune change.

Measurements

In a first measurement campaign three energy steps of $\Delta E = 4 \text{ MeV u}^{-1}$ were performed for carbon ion beams starting at $E_{\text{kin}} = 200 \text{ MeV u}^{-1}$. The $B\rho$ -curve of the dipoles was defined by a maximal ramp rate of $\frac{dI}{dt} = 2000 \text{ A s}^{-1}$. The ramp of all optic magnets (quadrupoles and chromaticity correction sextupoles) was advanced by 5 ms. In order to measure the tune shift achieved by the introduced ramp delay, we programmed custom waveforms to intermediate flat tops (including respective round-offs). The integrated fields for the bending dipoles and one quadrupole family were calculated from current waveform measurements, as illustrated in Fig. 2 for the first energy step. While further analysis and measurements are needed, tune measurements with a Schottky monitor [11], indicate that the tune returns to the initial value after the full ramp. During the energy change, specifically before the bending dipoles start their ramp, as shown in Fig. 5, a tune shift of $\Delta Q_x \approx 1.1 - 1.2 \times 10^{-3}$ was achieved. This is comparable to the expected tune shift $\Delta Q_x = 1.16 \times 10^{-3}$ for a modified PIMMS lattice with an change in $\delta k_1 = 0.8\%$ of k_1 in Eq. (4). Since in the measurements all optic magnets were ramped in advance the expected tune change for 0.8% is smaller than for 0.16% with only the focusing quadrupoles. In future measurements we will therefore focus on only adding an advanced gradient ramp for the focusing quadrupoles for faster energy changes.

SUMMARY AND OUTLOOK

In this contribution, we investigate strategies to enable fast energy changes for multi-energy extraction in ion beam therapy. We present a proposed workflow, validated through Xsuite simulations, along with initial measurements at MedAustron. Over the next year, we plan to expand this approach and integrate it with RFKO extraction of bunched beams.

ACKNOWLEDGMENTS

The financial support of the Austrian Ministry of Education, Science, and Research is gratefully acknowledged for providing beam time and research infrastructure at MedAustron. Furthermore, I would like to thank the TBU, NCR, and OPS departments at MedAustron, as well as the accelerator group at TU Wien for their support and scientific input.

REFERENCES

- [1] L. Badano *et al.*, “Proton-Ion Medical Machine Study (PIMMS), 1”, Rep., 2000. <https://cds.cern.ch/record/385378>
- [2] P. J. Bryant *et al.*, “Proton-Ion Medical Machine Study (PIMMS), 2”, Rep., 2000. <https://cds.cern.ch/record/449577>
- [3] I. Badano and S. Rossi, “Characteristics of a betatron core for extraction in a proton-ion medical synchrotron”, CERN, Geneva, Rep., 1997. <https://cds.cern.ch/record/2846932>
- [4] K. Noda *et al.*, “Slow beam extraction by a transverse RF field with AM and FM”, *Nucl. Instrum. Methods Phys. Res., Sect. A*, vol. 374, no. 2, pp. 269–277, 1996. [doi:10.1016/0168-9002\(96\)00096-4](https://doi.org/10.1016/0168-9002(96)00096-4)
- [5] A. D. Franco *et al.*, “Slow Extraction Optimization at the MedAustron Ion Therapy Center: Implementation of Front End Acceleration and RF Knock Out”, in *Proc. IPAC'18*, Vancouver, Canada, Apr.-May 2018, pp. 453–456. [doi:10.18429/JACoW-IPAC2018-MOPML025](https://doi.org/10.18429/JACoW-IPAC2018-MOPML025)
- [6] F. Kühteubl, “Slow extraction optimisation for the MedAustron synchrotron”, Technische Universität Wien, 2024. [doi:10.34726/hss.2024.88260](https://doi.org/10.34726/hss.2024.88260)
- [7] C. Schoemers *et al.*, “The intensity feedback system at Heidelberg Ion-Beam Therapy Centre”, *Nucl. Instrum. Methods Phys. Res., Sect. A*, vol. 795, pp. 92–99, 2015. [doi:10.1016/j.nima.2015.05.054](https://doi.org/10.1016/j.nima.2015.05.054)
- [8] G. Iadarola *et al.*, “Xsuite: An Integrated Beam Physics Simulation Framework”, *JACoW*, vol. HB2023, TUA2I1, 2024. [doi:10.18429/JACoW-HB2023-TUA2I1](https://doi.org/10.18429/JACoW-HB2023-TUA2I1)
- [9] Y. Kohayashi and H. Takahashi, “Improvement Of The Emittance In The Resonant Beam Ejection”, in *6th International Conference on High-Energy Accelerators*, pp. 347–351, 1967.
- [10] M. Q. Barton, “Beam Extraction from the Proton Synchrotron”, in *Proc. PAC'67*, Washington D.C., USA, pp. 660–666, Jun. 1967. [doi:10.1109/TNS.1967.4324635](https://doi.org/10.1109/TNS.1967.4324635)
- [11] F. Caspers, “Schottky signals for longitudinal and transverse bunched-beam diagnostics”, 2009. [doi:10.5170/CERN-2009-005.407](https://doi.org/10.5170/CERN-2009-005.407)